

# Resonant reflection of surface water waves by periodic sandbars

By CHIANG C. MEI

Department of Civil Engineering, Massachusetts Institute of Technology, Cambridge, MA 02139

(Received 15 June 1984 and in revised form 27 September 1984)

One of the possible mechanisms of forming offshore sandbars parallel to a coast is the wave-induced mass transport in the boundary layer near the sea bottom. For this mechanism to be effective, sufficient reflection must be present so that the waves are partially standing. The main part of this paper is to explain a theory that strong reflection can be induced by the sandbars themselves, once the so-called Bragg resonance condition is met. For constant mean depth and simple harmonic waves this resonance has been studied by Davies (1982), whose theory, is however, limited to weak reflection and fails at resonance. Comparison of the strong reflection theory with Heathershaw's (1982) experiments is made. Furthermore, if the incident waves are slightly detuned or slowly modulated in time, the scattering process is found to depend critically on whether the modulational frequency lies above or below a threshold frequency. The effects of mean beach slope are also studied. In addition, it is found for periodically modulated wave groups that nonlinear effects can radiate long waves over the bars far beyond the reach of the short waves themselves. Finally it is argued that the breakpoint bar of ordinary size formed by plunging breakers can provide enough reflection to initiate the first few bars, thereby setting the stage for resonant reflection for more bars.

---

## 1. Introduction

On natural beaches nearly periodic longshore sandbars can be found in bays or on open coasts. In a recent thesis on this topic, Dolan (1983) cites, for example, observations by Kindle (1936) and Dolan (1983) in Chesapeake Bay, Evans (1940) and Saylor & Hands (1970) in Lake Michigan, Lau & Travis (1973) in Escambia Bay, Florida, Sheppard (1950) on the Southern California coast and Short (1975) in the Alaskan Arctic. According to these references, multiple bars are usually located on very mild beaches (slope  $< 0.005$ ) on which plunging breakers are common. The number of bars can range from 3 to 17 (Chesapeake Bay). While the bar spacings vary widely (from 12 m in bays to 480 m on an open coast), they generally increase offshore with increasing depth. Because of the complexity of local variability of waves and currents and their interaction with sedimentary structures, it is unlikely that any single mechanism prevails at all these sites where definitive wave records are yet lacking (Dolan 1983). Perhaps the only established aspect of the whole process is the generation of the first bar on an initially barless beach. According to Evans (1940), it is the falling crest of the plunging breaker that stirs up sand particles and deposits them behind. Thus the first bar usually appears at the breaker line, and is therefore called the breakpoint bar, which is immediately followed by a trough on the shoreward side; this has been confirmed in the laboratory by Keulegan (1948).

The particular mechanism of mass transport in a wave-induced boundary layer

near the sea bottom has been known to be relevant to the movement of sediments. In particular, if there is a standing wave over an initially horizontal bottom, the Lagrangian drift near the bottom of the boundary layer converges toward the nodes and diverges from the antinodes, while the reverse is true near the top of the boundary layer. As a consequence, heavy particles rolling on the seabed tend to drift towards the nodes and light particles in suspension towards the antinodes. Therefore sandbars near a seawall have wavelength one-half of the dominant incident waves; this feature has been observed in the laboratory for some time (Bagnold 1948; Herbich, Murphy & Van Weele 1965; Carter, Liu & Mei 1973; Nielsen 1979) all for bottom of zero mean slope. For partially standing waves, Carter *et al.* have found from the theory of mass transport in a laminar boundary layer (Longuet-Higgins 1953) that the reflection coefficient must exceed the critical value of 0.414 for the Lagrangian drift to converge somewhere between the nodes and their adjacent antinodes. Under weaker reflection the mass transport and the mean particle drift are essentially unidirectional along the incident wave. Carter *et al.* have also confirmed these predictions by observing sparsely populated heavy particles on the smooth bottom of a wave tank. Since eddy-viscosity models for the bottom boundary layers do not alter the results of mass transport qualitatively for either progressive (Longuet-Higgins 1958) or standing (Johns 1970) waves, one may expect the same for the mass transport in the turbulent boundary layer beneath partially reflected waves and the associated effects on the initiation of sandbars; the threshold reflection coefficient may, of course, deviate somewhat from the laminar value 0.414. However, on natural beaches of mild slope, short waves are supposed to lose most of their energy by breaking, hence reflection at the shore is usually thought to be small. What, then, is the origin of reflection needed for the mass-transport mechanism? Carter *et al.* have earlier speculated without quantitative argument that the breakpoint bar caused by a plunging breaker can supply sufficient reflection. A complementary theory has been recently put forth by Davies (1982) that reflected waves can be resonated by equally spaced bars if the bar wavelength is one-half that of the incident waves.

This kind of resonant reflection is known as *Bragg reflection* in crystallography, and its possibility in water waves can be easily seen from the boundary condition on the bottom. Let  $h$  denote the mean depth, which is assumed by Davies to be a constant, and  $\delta(x)$  denote the bar height above the mean. For small bar amplitudes we have

$$\frac{\partial\phi}{\partial z} \approx \left( \delta \frac{\partial\phi}{\partial x} \right)_x \quad (z = -h), \quad (1.1)$$

where  $\phi$  is the wave potential. If the incident wave has the potential

$$-\frac{igA}{2\omega} \frac{\cosh k(z+h)}{\cosh kh} e^{ikx-i\omega t} + * \quad (1.2)$$

and the bottom is sinusoidal with half the wavelength,

$$\delta = \frac{1}{2}D(e^{2ikx} + e^{-2ikx}), \quad (1.3)$$

then the boundary condition (1.1) becomes approximately

$$\frac{\partial\phi}{\partial z} = ikD \frac{gkA}{4\omega \cosh kh} (-e^{-ikx-i\omega t} + 3e^{3ikx-i\omega t}) + * \quad (z = -h). \quad (1.4)$$

The first term in (1.4) will clearly resonate the reflected wave on the free surface. In fact this is a special case of three-wave resonance due to quadratic interaction. If the

three waves are described by  $a_j \exp i(\mathbf{k}_j \cdot \mathbf{x} - \omega_j t)$  the conditions for resonance are

$$\omega_1 \pm \omega_2 \pm \omega_3 = 0, \quad \mathbf{k}_1 \pm \mathbf{k}_2 \pm \mathbf{k}_3 = 0. \quad (1.5a, b)$$

Here we have simply  $\omega_1 = \omega_2 = \omega$ ,  $\omega_3 = 0$  and  $\mathbf{k}_1 = -\mathbf{k}_2 = \mathbf{k}_3 = k\mathbf{e}_1$ .

Experiments demonstrating this resonant reflection over sandbars have been reported by Heathershaw (1982). An implication of this finding is that, when there is a large patch of periodic sandbars, seaward reflection can be strong, which in turn causes new sand accumulation at half-wavelength intervals on the seaward side of the patch. The extended patch further enhances reflection and initiates more sandbars, until the depth becomes too great for waves to be felt at the bottom. This tendency of sediment transport has also been observed by Heathershaw by sprinkling sand on two sides of a fixed bar patch.

Being based on the technique of regular perturbations, Davies' theory is nevertheless valid only for infinitesimal reflection and away from resonance. Specifically, his reflection coefficient, defined as the ratio of the reflected wave amplitude to the incident wave amplitude, is given by

$$R = \frac{2kD}{\sinh 2kh + 2kh} \frac{2k}{l} \frac{|\sin(2k/l)m\pi|}{(2k/l)^2 - 1}, \quad (1.6)$$

where  $m$  is the number of sandbars and  $l$  their wavenumber. When  $2k/l \rightarrow 1$ , and  $m$  becomes large, the reflection coefficient becomes unbounded,

$$R \rightarrow \frac{2kD}{\sinh 2kh + 2kh} \frac{m\pi}{2}, \quad (1.7)$$

and this theory breaks down.

In this paper we shall give a theory appropriate for large reflection. Governing equations uniformly valid in space and time will be found which couple the incident and reflected wave envelopes through the bar amplitudes. Results for perfectly tuned waves on a bottom of zero mean slope will be compared to the experiments of Heathershaw. Effects of detuning will then be treated, also for zero mean slope; the results can be easily applied to periodically modulated wave groups. The existence of a cut-off frequency is pointed out. A simple case of parallel bars on a mildly sloping beach will be detailed. Finally nonlinear effects of bars on the second-order long waves caused by detuned or periodically modulated short waves will be discussed.

Prior to Davies, there exist papers on long waves over periodic topography in shallow water (McGoldrick 1968; Rhines & Bretherton 1973 for a rotating ocean). By regular perturbations these authors deduced the Mathieu equation, and only indicated that resonant reflection corresponded to a subharmonic instability. They did not give a uniformly valid theory at resonance. Motivated by the work of Davies (1982), Mitra & Greenberg (1984) have considered an infinite patch of periodic sandbars on a constant mean depth and studied the slow evolution of reflected waves with respect to time but not to space. Their theory can therefore not be compared with the finite-patch experiment of Heathershaw. On the other hand, in X-ray diffraction by crystals the linear theory is very well developed (see e.g. Pinsker 1978). It turns out that the equations governing time-invariant two-dimensional diffraction of X-rays in a deformed crystal resemble, but are not the same as, those for water waves over sandbars on a mildly sloping beach. Problems of physical interest in X-ray diffraction are, however, not altogether similar to those in water waves. This is particularly so in regard to nonlinear effects, which appear to be less studied in the former field.

## 2. Approximate equations for wave envelopes

We shall first derive the asymptotic equations applicable for spatially periodic sandbars on an otherwise mildly sloping bottom. The waves are assumed to be small in amplitude so that nonlinearity (especially breaking) is unimportant. The incident waves are allowed to be slowly modulated in time and space. The slopes of the free surface, the mean bottom, the sandbars and the ratio of wavelength to group length are all assumed to be characterized by the same small parameter  $\epsilon$ . To the accuracy needed, it can be shown that nonlinearity on the free surface does not affect the leading-order results, and it suffices to begin with the governing equations, which are linearized with respect to both the mean free surface and the mean sea bottom. The velocity potential must satisfy

$$\nabla^2 \phi + \phi_{zz} = 0 \quad (-h < z < 0) \quad (2.1)$$

in the fluid, where  $h(x, y)$  is the mean depth and

$$\nabla = \left( \frac{\partial}{\partial x}, \frac{\partial}{\partial y} \right) \quad (2.2)$$

is the horizontal gradient operator. The linearized kinematic and dynamic conditions on the free surface can be combined to give

$$g\phi_z + \phi_{tt} = 0 \quad (z = 0). \quad (2.3)$$

On the sea bottom, vanishing of the normal velocity leads to

$$\phi_z = -\nabla h \cdot \nabla \phi + \epsilon \nabla \cdot (\delta \nabla \phi) + O(\epsilon^2) \quad (z = -h). \quad (2.4)$$

We introduce the slow variables  $\bar{x} = \epsilon x$ ,  $\bar{y} = \epsilon y$  and  $\bar{t} = \epsilon t$ , and the multiple-scale expansions

$$\phi = \epsilon \phi^{(1)} + \epsilon^2 \phi^{(2)} + O(\epsilon^3), \quad (2.5)$$

where  $\phi^{(1)} = \phi^{(1)}(x, y, z, t, \bar{x}, \bar{y}, \bar{t})$  etc. The perturbation equations at  $O(\epsilon)$  are

$$\nabla^2 \phi^{(1)} + \phi_{zz}^{(1)} = 0 \quad (-h < z < 0), \quad (2.6)$$

$$g\phi_z^{(1)} + \phi_{tt}^{(1)} = 0 \quad (z = 0), \quad (2.7)$$

$$\phi_z^{(1)} = 0 \quad (z = -h). \quad (2.8)$$

At  $O(\epsilon^2)$  we have

$$\nabla^2 \phi^{(2)} + \phi_{zz}^{(2)} = -(\nabla \cdot \bar{\nabla} + \bar{\nabla} \cdot \nabla) \phi^{(1)} \quad (-h < z < 0), \quad (2.9)$$

$$\phi_{tt}^{(2)} + g\phi_z^{(2)} = -\frac{\partial^2 \phi^{(1)}}{\partial \bar{t} \partial \bar{t}} \quad (z = 0), \quad (2.10)$$

$$\phi_z^{(2)} = -\bar{\nabla} H \cdot \nabla \phi^{(1)} + \nabla \cdot (\delta \nabla \phi^{(1)}) \quad (z = -h), \quad (2.11)$$

where

$$\bar{\nabla} = \left( \frac{\partial}{\partial \bar{x}}, \frac{\partial}{\partial \bar{y}} \right). \quad (2.12)$$

Employing the idea of ray approximation (see e.g. Mei 1983), we take the first-order potential  $\phi^{(1)}$  to be

$$\phi^{(1)} = \psi^+ e^{iS^+} + * + \psi^- e^{iS^-} + *. \quad (2.13)$$

Here the superscripts + and - refer respectively to incident and reflected waves,  $\psi^+$  and  $\psi^-$  are the corresponding vertical profiles:

$$\psi^\pm = -\frac{ig \cosh k(z+h)}{2\omega \cosh kh} A^\pm. \quad (2.14)$$

$A^+$  and  $A^-$  are the complex wave amplitudes, and  $S^+$  and  $S^-$  are the phases.

From here on we only consider the case where the mean bottom contours are parallel to the  $y$ -axis, i.e.  $h = h(\bar{x})$ ; thus

$$S^\pm = \pm \int^x \alpha(\bar{x}) dx + \beta y - \omega t. \quad (2.15)$$

The wavenumber vectors are

$$\mathbf{k}^\pm = (\pm \alpha, \beta), \quad (2.16)$$

with

$$\alpha = k \cos \theta, \quad \beta = k \sin \theta = \text{constant}, \quad (2.17)$$

where  $\theta$  is the local inclination of the incident wave with respect to the  $x$ -axis. The magnitude  $k$  of both  $\mathbf{k}^+$  and  $\mathbf{k}^-$  satisfies the familiar dispersion relation

$$\omega^2 = gk \tanh kh \quad (2.18)$$

at leading order. Note that the reflected waves are permitted to be of the *same* order as the incident wave, in anticipation of resonance.

Substituting (2.13) into (2.9)–(2.11), we get

$$\begin{aligned} \nabla^2 \phi^{(2)} + \phi_{zz}^{(2)} = & -i[\mathbf{k}^+ \cdot \bar{\nabla} \psi^+ + \bar{\nabla} \cdot (\mathbf{k}^+ \psi^+)] e^{iS^+} + * \\ & -i[\mathbf{k}^- \cdot \bar{\nabla} \psi^- + \bar{\nabla} \cdot (\mathbf{k}^- \psi^-)] e^{iS^-} + * \quad (-h < z < 0) \end{aligned} \quad (2.19)$$

and

$$g\phi_z^{(2)} + \phi_{tt}^{(2)} = 2i\omega \left( \frac{\partial \psi^+}{\partial t} e^{iS^+} + \frac{\partial \psi^-}{\partial t} e^{iS^-} \right) + * \quad (z = 0). \quad (2.20)$$

We assume the sandbars to be parallel to the  $y$ -axis and spaced at one-half of the local wavelength:

$$\delta = \frac{1}{2}D \left[ \exp\left(2i \int \alpha dx\right) + \exp\left(-2i \int \alpha dx\right) \right], \quad (2.21)$$

where the real amplitude  $D(\bar{x}, \bar{y})$  can vary slowly in both horizontal directions. It then follows from (2.11) that

$$\begin{aligned} \phi_z^{(2)} = & -i\bar{\nabla} h \cdot (\mathbf{k}^+ \psi^+ e^{iS^+} + \mathbf{k}^- \psi^- e^{iS^-}) + * + \frac{1}{2}D(\alpha^2 - \beta^2) (\psi^- e^{iS^+} + \psi^+ e^{iS^-}) \\ & + * + \dots \quad (z = -h). \end{aligned} \quad (2.22)$$

Only the terms with the phases  $S^+$  and  $S^-$  are kept, as other terms do not force resonance (cf. (1.4)). If the potential  $\phi^{(2)}$  is expressed as

$$\phi^{(2)} = i\gamma^+ e^{iS^+} + * + i\gamma^- e^{-iS^-} + * + \dots \quad (2.23)$$

the conditions for  $\gamma^+$  are

$$\gamma_{zz}^+ - k^2 \gamma^+ = \mathbf{k}^+ \cdot \bar{\nabla} \psi^+ + \bar{\nabla} \cdot (\mathbf{k}^+ \psi^+) \quad (-h < z < 0), \quad (2.24)$$

$$\gamma_z^+ - \frac{\omega^2}{g} \gamma^+ = -\frac{2\omega}{g} \psi_t^+ \quad (z = 0), \quad (2.25)$$

$$\gamma_z^+ = \bar{\nabla} h \cdot (\mathbf{k}^+ \psi^+) + \frac{1}{2}iD(\alpha^2 - \beta^2) \psi^- \quad (z = -h). \quad (2.26)$$

$\psi^-$  satisfies a similar set of equations if the superscripts + and - are interchanged.

Note that  $\psi^\pm$  are the homogeneous solutions of (2.24)–(2.26). Multiplying (2.24) by  $(\psi^+)^*$  and the conjugate equation by  $\psi^+$ , and then integrating the difference, we get a solvability condition for  $\gamma^+$ , which can be reduced to

$$\bar{\nabla} \cdot C_g^+ \frac{A^{+2}}{2} + \frac{\partial}{\partial t} \frac{A^{+2}}{2} = -\frac{i}{2} \Omega_0 (A^+)^* A^- \cos 2\theta + *, \quad (2.27)$$

By an analogous argument we also get

$$\bar{\nabla} \cdot C_g^- \frac{A^{-2}}{2} + \frac{\partial}{\partial t} \frac{A^{-2}}{2} = +\frac{i}{2} \Omega_0 (A^+)^* A^- \cos 2\theta + *, \quad (2.28)$$

where

$$C_g^\pm = \frac{k^\pm}{k} \frac{\omega}{2k} \left( 1 + \frac{2kh}{\sinh 2kh} \right) \quad (2.29)$$

are the group velocities and

$$\Omega_0 = \frac{gk^2 D}{4\omega \cosh^2 kh} = \frac{\omega k D}{2 \sinh 2kh}. \quad (2.30)$$

Note that  $\Omega_0$  has the dimension of frequency; it increases with  $kD$ , but decreases with  $kh$ . Equations (2.27) and (2.28) are modifications of the well-known laws of wave-action conservation. Clearly

$$\frac{\partial}{\partial t} (|A^+|^2 + |A^-|^2) + \bar{\nabla} \cdot (C_g^+ |A^+|^2 + C_g^- |A^-|^2) = 0. \quad (2.31)$$

Thus sandbars can transfer energy between incident and reflected waves. Alternatively we can repeat the above procedure by replacing  $(\psi^\pm)^*$  with  $\psi^\pm$  and obtain

$$\bar{\nabla} \cdot C_g^\pm \frac{(A^\pm)^2}{2} + \frac{\partial}{\partial t} \frac{(A^\pm)^2}{2} = -i \Omega_0 A^+ A^- \cos 2\theta. \quad (2.32)$$

They can also be written as

$$\frac{\partial A^+}{\partial t} + C_{g_1}^+ \bar{\nabla} A^+ + (\bar{\nabla} \cdot C_g^+) \frac{A^+}{2} = -i \Omega_0 \cos 2\theta A^- \quad (2.33)$$

and

$$\frac{\partial A^-}{\partial t} + C_{g_1}^- \bar{\nabla} A^- + (\bar{\nabla} \cdot C_g^-) \frac{A^-}{2} = -i \Omega_0 \cos 2\theta A^+. \quad (2.34)$$

It is evident that the coupling of  $A^+$  and  $A^-$  is stronger if the bars are higher and/or if the angle of incidence is further away from  $45^\circ$ . Since all subsequent discussions will be for the long-scale variations only, there is no need to distinguish  $\bar{x}$ ,  $\bar{y}$ ,  $\bar{t}$  from  $x$ ,  $y$ ,  $t$ ; all overbars will be omitted from here on. Also for brevity we shall make the following change of notation:

$$A^+ = A, \quad A^- = B. \quad (2.35)$$

Thus (2.33) and (2.34) become

$$\frac{\partial A}{\partial t} + C_{g_1} \frac{\partial A}{\partial x} + C_{g_2} \frac{\partial A}{\partial y} + \frac{\partial C_{g_1}}{\partial x} \frac{A}{2} = -i \Omega_0 \cos 2\theta B, \quad (2.36)$$

$$\frac{\partial B}{\partial t} - C_{g_1} \frac{\partial B}{\partial x} + C_{g_2} \frac{\partial B}{\partial y} - \frac{\partial C_{g_1}}{\partial x} \frac{B}{2} = -i \Omega_0 \cos 2\theta A, \quad (2.37)$$

where

$$\begin{aligned} (C_{g_1}, C_{g_2}) &= (\alpha, \beta) C_g / k \\ &= C_g (\cos \theta, \sin \theta). \end{aligned} \quad (2.38)$$

Also, in the time-invariant limit ( $\partial/\partial t = 0$ ), (2.36) and (2.37) resemble, but are not identical to, those in X-ray diffraction by deformed crystals, first given by Tagaki (1969; for other relevant topics see also Pinsker 1978).

For the special case of constant mean depth ( $h = \text{const}$ ), (2.36) and (2.37) can be combined to give

$$\left[ \left( \frac{\partial}{\partial t} + C_{g_2} \frac{\partial}{\partial y} \right)^2 - C_{g_1}^2 \frac{\partial^2}{\partial x^2} + \Omega_0^2 \cos^2 2\theta \right] \begin{Bmatrix} A \\ B \end{Bmatrix} = 0. \quad (2.39)$$

If we restrict further to normal incidence

$$\theta = \frac{\partial}{\partial y} = 0, \quad (2.40)$$

(2.39) reduces to 
$$\left( \frac{\partial^2}{\partial t^2} - C_g^2 \frac{\partial^2}{\partial x^2} + \Omega_0^2 \right) \begin{Bmatrix} A \\ B \end{Bmatrix} = 0, \quad (2.41)$$

which is the Klein–Gordon equation well known in quantum mechanics and in the vibration of elastically supported strings. It is easy to see from (2.39) that the envelopes behave as dispersive waves. In contrast, we recall that in water of constant or infinite depth, dispersive effects in the envelope are important only for much longer distances ( $O(\epsilon^{-2}k)$ ) or time ( $O(\epsilon^{-2}\omega)$ ). It is worth noting that the evolution equations for three-wave resonance in a homogeneous medium due to quadratic interaction reduces to (2.36) and (2.37) with constant  $C_g$ , when one of the three waves is assumed to have constant amplitude. This assumption is called the pump-wave approximation in plasma physics (see e.g. Craik & Adam 1978).

If we further restrict to bars uniformly distributed over the entire horizontal plane, all spatial derivatives in these equations vanish; the results of Mitra & Greenberg ((37) and (38)) follow readily.

### 3. Normal incidence of a detuned wavetrain over a bar patch

Consider the normal incidence of a periodic wavetrain arriving from  $x \sim -\infty$ . Periodic bars of constant amplitude  $D$  and wavenumber  $2k$  are present in the range  $0 < x < L$ . The mean depth  $h$  is constant. Let the incident wave be slightly detuned from Bragg resonance so that its wavenumber is  $k + \epsilon K$ , where  $K$  is of order unity. The detuning implies a frequency deviation by the amount  $\epsilon\Omega$ , where

$$\Omega = C_g K. \quad (3.1)$$

The incident-wave potential is given by (2.13) and (2.14) with the + superscript and the amplitude

$$A^+ = A = A_0 e^{i(Kx - \Omega t)} \quad (x < 0), \quad (3.2)$$

where  $x$  and  $t$  are slow coordinates. The differential equations for  $x < 0$  and  $x > L$  are

$$\left( \frac{\partial}{\partial t} + C_g \frac{\partial}{\partial x} \right) A = 0 \quad (x < 0, x > L), \quad (3.3)$$

$$\left( \frac{\partial}{\partial t} - C_g \frac{\partial}{\partial x} \right) B = 0 \quad (x < 0). \quad (3.4a)$$

We impose the condition that there be no reflected waves on the side  $x > L$ :

$$B = 0 \quad (x > L). \quad (3.4b)$$

Over the bars  $0 < x < L$  we have

$$\frac{\partial A}{\partial t} + C_g \frac{\partial A}{\partial x} = -i\Omega_0 B, \quad (3.5)$$

$$\frac{\partial B}{\partial t} - C_g \frac{\partial B}{\partial x} = -i\Omega_0 A. \quad (3.6)$$

Continuity of  $A$  and  $B$  at  $x = 0$  and  $L$  gives four conditions. The solution in all three regions can be readily found.† Four cases may be distinguished with respect to the cutoff frequency  $\Omega_0$ .

*Case (i):  $\Omega > \Omega_0$*

Here the detuning frequency is above cutoff. Over the bars,  $0 < x < L$ , the envelope wavenumber  $P$  is given by

$$PC_g = (\Omega^2 - \Omega_0^2)^{\frac{1}{2}}, \quad (3.7)$$

and the two envelopes vary according to

$$A = A_0 T(x) e^{-i\Omega t}, \quad (3.8a)$$

where 
$$T(x) = \frac{PC_g \cos P(L-x) - i\Omega \sin P(L-x)}{PC_g \cos PL - i\Omega \sin PL} \quad (3.8b)$$

and 
$$B = A_0 R(x) e^{-i\Omega t}, \quad (3.9a)$$

with 
$$R(x) = \frac{-i\Omega_0 \sin P(L-x)}{PC_g \cos PL - i\Omega \sin PL}. \quad (3.9b)$$

On the incidence side,  $x < 0$ ,

$$A = A_0 e^{iKx - i\Omega t}, \quad B = A_0 R(0) e^{-iKx - i\Omega t}. \quad (3.10)$$

We define the reflection coefficient to be

$$R(0) = \frac{-i\Omega_0 \sin PL}{PC_g \cos PL - i\Omega \sin PL}. \quad (3.11)$$

On the transmission side,  $x > L$ ,

$$A = A_0 T(L) e^{iKx - i\Omega t}, \quad B = 0. \quad (3.12)$$

The transmission coefficient is defined to be

$$T(L) = \frac{PC_g}{PC_g \cos PL - i\Omega \sin PL}. \quad (3.13)$$

The reflected wave intensity over the bars is

$$|R(x)|^2 = \frac{\sin^2 \left\{ \frac{\Omega_0 L}{C_g} \left[ \left( \frac{\Omega}{\Omega_0} \right)^2 - 1 \right]^{\frac{1}{2}} \left( 1 - \frac{x}{L} \right) \right\}}{\left( \frac{\Omega}{\Omega_0} \right)^2 - \cos^2 \left\{ \frac{\Omega_0 L}{C_g} \left[ \left( \frac{\Omega}{\Omega_0} \right)^2 - 1 \right]^{\frac{1}{2}} \right\}}. \quad (3.14)$$

† Craik & Adam (1978) have given mathematical solutions similar to ours in the context of pump-wave approximation of three-wave resonance.



Its value at  $x = 0$  can be written in a form which also appears in the Bragg reflection of X-rays by a crystal of finite thickness (Pinsker 1978, p. 255):

$$|R(0)|^2 = \left\{ \left( \frac{\Omega}{\Omega_0} \right)^2 + \left[ \left( \frac{\Omega}{\Omega_0} \right)^2 - 1 \right] \cot^2 \frac{\Omega_0 L}{C_g} \left[ \left( \frac{\Omega}{\Omega_0} \right)^2 - 1 \right]^{\frac{1}{2}} \right\}^{-1}. \quad (3.15)$$

Case (ii):  $0 < \Omega < \Omega_0$

The detuning frequency is below cutoff; the envelope varies exponentially in  $x$  for  $0 < x < L$ . Denoting

$$Q = iP, \quad \text{where} \quad QC_g = (\Omega_0^2 - \Omega^2)^{\frac{1}{2}}, \quad (3.16)$$

we get from (3.7)

$$T(x) = \frac{iQC_g \cosh Q(L-x) + \Omega \sinh Q(L-x)}{iQC_g \cosh QL + \Omega \sinh QL}, \quad (3.17)$$

$$R(x) = \frac{\Omega_0 \sinh Q(L-x)}{iQC_g \cosh QL + \Omega \sinh QL} \quad (3.18)$$

for  $0 < x < L$ . Envelopes outside the bar region are given by (3.10) and (3.12), with  $R(0)$  and  $T(L)$  evaluated from (3.17) and (3.18).

The reflected-wave intensity over the bars is

$$|R(x)|^2 = \frac{\sinh^2 \left\{ \frac{\Omega_0 L}{C_g} \left[ 1 - \left( \frac{\Omega}{\Omega_0} \right)^2 \right]^{\frac{1}{2}} \left( 1 - \frac{x}{L} \right) \right\}}{\cosh^2 \left\{ \frac{\Omega_0 L}{C_g} \left[ 1 - \left( \frac{\Omega}{\Omega_0} \right)^2 \right]^{\frac{1}{2}} \right\} - \left( \frac{\Omega}{\Omega_0} \right)^2}. \quad (3.19)$$

Case (iii):  $\Omega = 0$  (perfect tuning)

The special limit of  $\Omega = 0$  corresponds to perfect tuning. Now  $Q$  in (3.16) reduces to  $K$  while

$$\frac{A}{A_0} = T(x) = \frac{\cosh \frac{\Omega_0}{C_g} (L-x)}{\cosh \frac{\Omega_0 L}{C_g}} \quad (0 < x < L), \quad (3.20)$$

$$\frac{B}{A_0} = R(x) = \frac{-i \sinh \frac{\Omega_0}{C_g} (L-x)}{\cosh \frac{\Omega_0 L}{C_g}} \quad (0 < x < L). \quad (3.21)$$

The dimensionless parameter  $\Omega_0 L/C_g$  may be written

$$\frac{\Omega_0 L}{C_g} = \frac{k^2 DL}{2kh + \sinh 2kh}, \quad (3.22)$$

which increases with the bar slope  $kD$  or the width of the bar patch, but decreases with increasing water depth. In very shallow water it reduces to

$$\frac{\Omega_0 L}{C_g} \rightarrow \frac{kL}{4} \frac{D}{h} \quad (kH \ll 1). \quad (3.23)$$

As the width  $L$  of the bar patch increases,  $R(0) \rightarrow -i$  and  $T \rightarrow 0$ ; there is complete reflection.

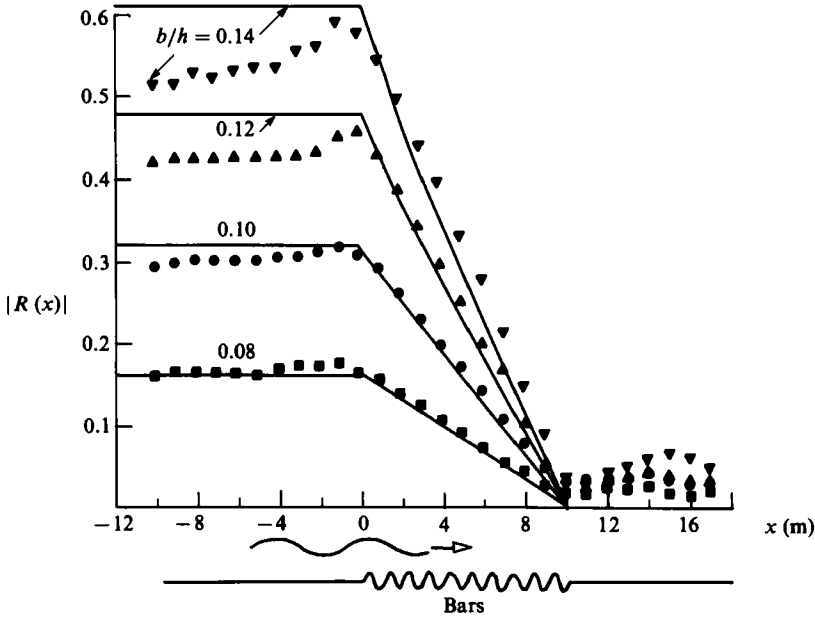


FIGURE 1. Comparison between theory (equation (3.9)) and experiments by Heathershaw (1982).  $b \equiv$  bar amplitude;  $x \equiv$  distance in metres along the direction of incident waves. The periodic bars are from  $x = 0$  to  $x = 10$  m.

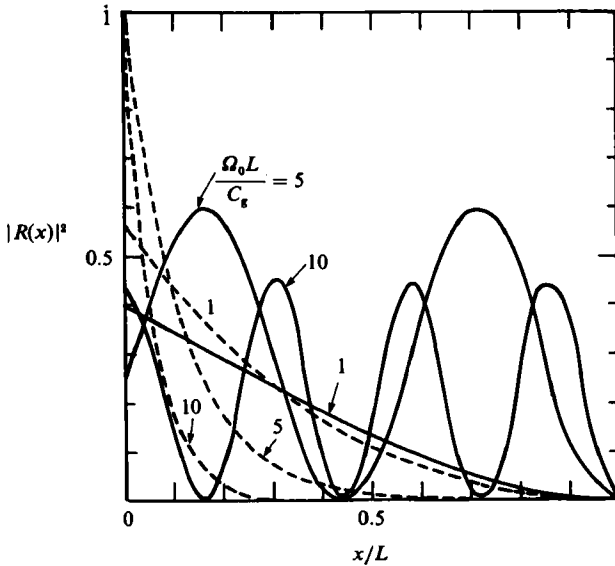


FIGURE 2. Reflection intensity over the sandbars. Normal incidence. Numbers by the curves give  $\Omega_0 L / C_g$ . —,  $\Omega / \Omega_0 = 0.5$ ; ----,  $\Omega / \Omega_0 = 1.5$ .

The results of this special case may now be compared with the experiments by Heathershaw (1982), who installed on the bottom of a long tank 10 sinusoidal bars of amplitude  $D = 5$  cm and wavelength 100 cm. Free-surface amplitudes were measured for several water depths, but for the same incident wavelength ( $2\pi/k = 200$  cm). In figure 1 the measured amplitudes of the reflected waves for the

region  $-10 \text{ m} < x < 17 \text{ m}$  are reproduced and compared with (3.8). The agreement is seen to be very good. Outside the patch our theory gives constant values that are less than the observed data. On the transmission side the small discrepancy is probably due to reflection from the beach. On the reflection side the discrepancy is greater for the shallower water and stronger reflection, suggesting that nonlinearity or reflection from the wavemaker may be significant.

For this special case of  $\Omega = 0$  it is straightforward to add the second-order correction associated with  $\phi^{(2)}$ ; the result is

$$\frac{B(x)}{A_0} = R(x) = \left[ -i \sinh \frac{\Omega_0}{C_g} (L-x) + M \cosh \frac{\Omega_0}{C_g} (L-x) \right] \operatorname{sech} \frac{\Omega_0 L}{C_g}, \quad (3.24)$$

where 
$$M = \frac{kD}{2} \tanh kh \frac{\sinh 2kh}{\sinh 2kh + 2kh}. \quad (3.25)$$

Since the correction is  $\frac{1}{2}\pi$  out of phase with the  $O(1)$  term, its effect on the magnitude of the reflection coefficient is  $O(\epsilon^2)$  and is quite negligible.

Case (iv):  $\Omega = \Omega_0$

At the cutoff frequency we take  $Q \rightarrow 0$  in (3.17) and (3.18) to get

$$T(x) = \frac{1 - i\Omega_0(L-x)/C_g}{1 - i\Omega_0 L/C_g}, \quad (3.26)$$

$$R(x) = \frac{-i\Omega_0(L-x)/C_g}{1 - i\Omega_0 L/C_g} \quad (3.27)$$

for  $0 < x < L$ . Note that in this case  $T(L) + R(0) = 1$ .

We now present theoretical results for detuned waves  $\Omega \neq 0$ .

In figure 2 the variation of the reflected-wave intensity over the sandbars is shown for  $\Omega/\Omega_0 = 0.5$  and  $1.5$  and for different widths of the bar patch. Below cutoff the variation is monotonic; above cutoff oscillatory. The case  $\Omega/\Omega_0 = 1$  is simple and is not plotted.

In figure 3 the reflected-wave intensity at  $x = 0$  is plotted as a function of  $\Omega_0 L/C_g$  for several values of  $\Omega/\Omega_0$ . Figure 4 shows  $|R(0)|^2$  as a function of  $\Omega/\Omega_0$  for several  $\Omega_0 L/C_g$ . Below cutoff  $|R(0)|^2$  rises to unity rapidly and monotonically as  $\Omega_0 L/C_g$  increases, implying nearly complete reflection. Above cutoff  $|R(0)|^2$  is oscillatory and attenuating in  $\Omega_0 L/C_g$ . Perfect transmission (zero reflection) occurs at the zeros of

$$\sin \frac{\Omega_0 L}{C_g} \left[ \left( \frac{\Omega}{\Omega_0} \right)^2 - 1 \right]^{\frac{1}{2}} = 0, \quad (3.28)$$

i.e. 
$$L = \frac{C_g}{\Omega_0} \frac{n\pi}{\left[ \left( \frac{\Omega}{\Omega_0} \right)^2 - 1 \right]^{\frac{1}{2}}} \quad (n = 1, 2, 3, \dots). \quad (3.29)$$

The limiting case of a semi-infinite bar patch ( $L \rightarrow \infty$ ) can be solved directly. The results are as follows.

For  $\Omega/\Omega_0 > 1$

$$\begin{Bmatrix} A \\ B \end{Bmatrix} = A_0 \begin{Bmatrix} 1 \\ R \end{Bmatrix} e^{iPx - i\Omega t} \quad (0 < x < \infty), \quad (3.30)$$

where 
$$R = \left\{ \frac{\Omega}{\Omega_0} + \left[ \left( \frac{\Omega}{\Omega_0} \right)^2 - 1 \right]^{\frac{1}{2}} \right\}^{-1}. \quad (3.31)$$

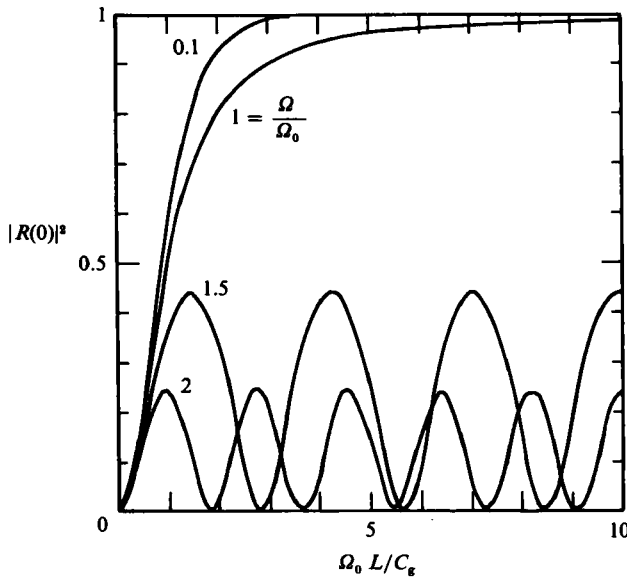


FIGURE 3. Reflection intensity at  $x = 0$  and for  $x < 0$ . Normal incidence.

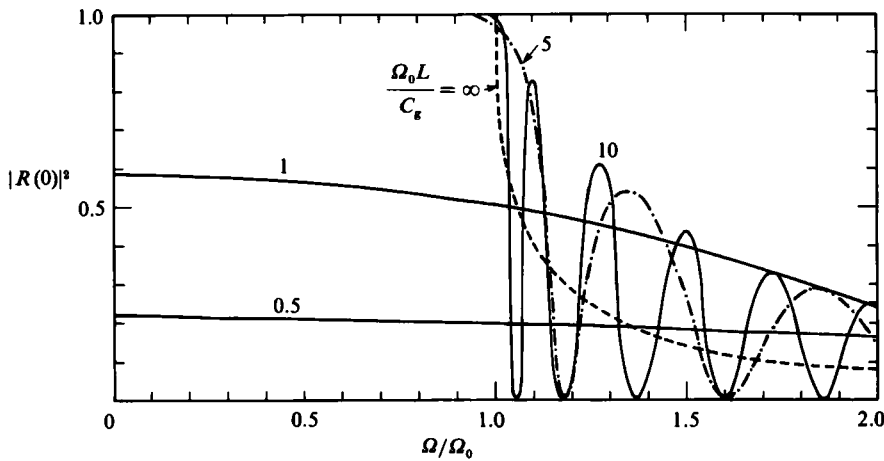


FIGURE 4. Reflection intensity at  $x = 0$  and for  $x < 0$ . Normal incidence.

Note that  $B$  propagates from left to right, opposite to the short waves enveloped by it. The propagation speed of  $A$  and  $B$  is

$$C_g \Omega (\Omega^2 - \Omega_0^2)^{\frac{1}{2}}, \tag{3.32}$$

which is always higher than  $C_g$  and approaches  $C_g$  as  $\Omega / \Omega_0 \rightarrow \infty$ .

For  $0 < \Omega / \Omega_0 < 1$

$$\begin{Bmatrix} A \\ B \end{Bmatrix} = A_0 \begin{Bmatrix} 1 \\ R \end{Bmatrix} e^{-Qx - i\Omega t} \quad (0 < x < \infty), \tag{3.33}$$

where

$$R = \left\{ \frac{\Omega}{\Omega_0} + i \left[ 1 - \left( \frac{\Omega}{\Omega_0} \right)^2 \right]^{\frac{1}{2}} \right\}^{-1}, \tag{3.34}$$

whose magnitude is unity, implying complete reflection. Thus short waves are trapped near the incidence edge of the bar field, with the penetration distance

$$Q^{-1} = C_g / \Omega_0 \left[ 1 - \left( \frac{\Omega}{\Omega_0} \right)^2 \right]^{\frac{1}{2}} = \left\{ K \left[ 1 - \left( \frac{\Omega}{\Omega_0} \right)^2 \right]^{\frac{1}{2}} \right\}^{-1}, \quad (3.35)$$

which is greater than the group length  $K^{-1}$  in the incidence zone.

Note that (3.34) is the limit of (3.18) for  $L \rightarrow \infty$ . However, (3.31) is not the limit of (3.9b). Mathematically, since any time-harmonic response is really the quasi-steady-state limit of an initial-value problem, the discrepancy merely indicates that the two limiting processes of  $L \rightarrow \infty$  and  $t \rightarrow \infty$  cannot be interchanged. Physically, when  $\Omega/\Omega_0 < 1$ ,  $A$  and  $B$  are wavelike. Setting  $L \rightarrow \infty$  at the outset (i.e. (3.31)) means that we seek the steady state without ever allowing reflection from  $x = L$ ; therefore it corresponds to  $\lim_{t \rightarrow \infty} \lim_{L \rightarrow \infty}$ . On the other hand, the  $\Omega_0 L/C_g \rightarrow \infty$  limit of (3.9b) corresponds to  $\lim_{L \rightarrow \infty} \lim_{t \rightarrow \infty}$ , which allows steady reflection from  $x = L$ .

So far all our results are for one train of detuned waves. An incident sea with a narrow-banded spectrum can be modelled crudely by two trains of detuned waves:

$$A = A_0 e^{iKx - i\Omega t} + \bar{A}_0 e^{-iKx + i\Omega t}, \quad (3.36)$$

where  $A_0$  and  $\bar{A}_0$  can in general be different. Because of linearity, the responses to  $A_0$  and  $\bar{A}_0$  can be separately treated. Let  $\bar{A}$  and  $\bar{B}$  denote respectively the envelopes of right-going and left-going waves over the bars  $0 < x < L$ . If we write

$$\left. \begin{aligned} \bar{A} &= \bar{A}_0 T^*(x) e^{-i\Omega t}, \\ \bar{B} &= \bar{A}_0 R^*(x) e^{-i\Omega t} \end{aligned} \right\} \quad (3.37)$$

it is easily seen from (3.5) and (3.6) that  $T^*$  and  $R^*$  are the complex conjugates of  $T$  and  $R$ , given respectively by (3.8b) and (3.9b). Therefore results for periodically modulated wave groups can be easily inferred and need not be discussed here. More realistic modelling of sea waves by accounting for randomness may reveal new features, however, and is worth while.

#### 4. Oblique incidence of slightly detuned waves

Consider first a sandbar field of infinite extent in a sea of constant mean depth, and envelopes of the type

$$\begin{Bmatrix} A \\ B \end{Bmatrix} = \begin{Bmatrix} A_0 \\ B_0 \end{Bmatrix} \exp i(px + qy - \Omega t) \quad (|x|, |y| < \infty). \quad (4.1)$$

Note first that the envelope wavenumber vector  $(p, q)$  need not in general be parallel to that of the short waves  $(\alpha, \beta)$ . The dispersion relation is

$$(\Omega - C_g q \sin \theta)^2 - (C_g p \cos \theta)^2 = \Omega_0^2 \cos^2 2\theta. \quad (4.2)$$

For fixed  $\Omega$  and  $\theta$  the above relation is represented by two branches of a hyperbola in the  $(p, q)$ -plane as shown in figure 5. Each branch becomes narrower for smaller  $\theta$ . For a fixed  $q$  satisfying the criterion

$$\left| q - \frac{\Omega}{C_g \sin \theta} \right| > \frac{\Omega_0 \cos 2\theta}{C_g \sin \theta} \quad (4.3)$$

two real values of  $p$  ( $+p, -p$ ), and hence two propagating envelopes, exist. Otherwise  $p$  is imaginary; the corresponding  $A$  and  $B$  are exponential (evanescent) in the

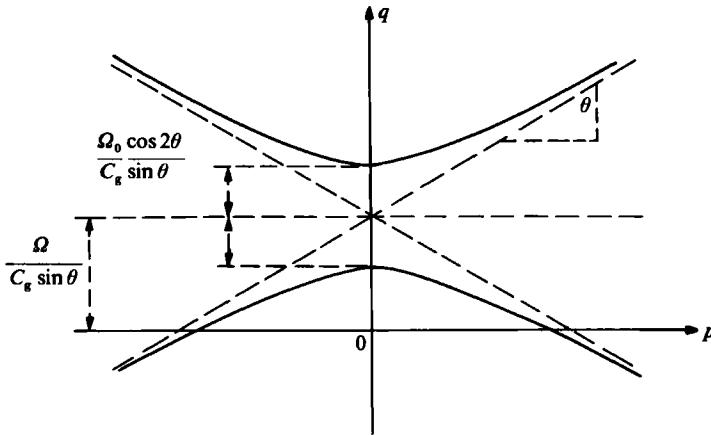


FIGURE 5. Dispersion relation for oblique waves on periodic bars.

$x$ -direction. If, instead,  $p$  is real and given, there are two possible values of  $q$ , corresponding to two different directions and wavenumbers. In the same direction two wavenumbers are also possible.

Consider now a bar field occupying the region  $0 < x < \infty$ . A sinusoidal envelope

$$A = A_0 \exp i [K(x \cos \theta + y \sin \theta) - \Omega t] \quad (x < 0) \quad (4.4)$$

arrives from  $x \rightarrow -\infty$  along the same direction as the waves in the envelope. The reflected envelope must be

$$B = B_0 \exp i [K(-x \cos \theta + y \sin \theta) - \Omega t] \quad (x < 0) \quad (4.5)$$

to the left of the bars. Over the bars the transmitted and reflected envelopes are

$$\begin{Bmatrix} A \\ B \end{Bmatrix} = \begin{Bmatrix} A_0 \\ B_0 \end{Bmatrix} \exp i (px + Ky \sin \theta - \Omega t) \quad (x > 0). \quad (4.6)$$

From (4.2) we get

$$(pC_g)^2 = \Omega_0^2 \cos^2 \theta \left[ \left( \frac{\Omega}{\Omega_0} \right)^2 - \left( \frac{\cos 2\theta}{\cos^2 \theta} \right)^2 \right], \quad (4.7)$$

where use has been made of (3.1). The cutoff frequency is now at

$$\Omega_0 \frac{\cos 2\theta}{\cos^2 \theta}, \quad (4.8)$$

above which  $A$  and  $B$  propagate to the right and below which both are evanescent. The directional dependence  $\cos 2\theta / \cos^2 \theta$  varies from 1 to  $-\infty$  as  $\theta$  increases from 0 to  $\frac{3}{4}\pi$  (see figure 6). From (2.37) the reflected envelope has the following magnitude:

$$R = \frac{B_0}{A_0} = \frac{\cos^2 \theta}{\cos 2\theta} \left\{ \frac{\Omega}{\Omega_0} - \left[ \left( \frac{\Omega}{\Omega_0} \right)^2 - \left( \frac{\cos 2\theta}{\cos^2 \theta} \right)^2 \right]^{\frac{1}{2}} \right\}. \quad (4.9)$$

Its dependences on  $\Omega / \Omega_0$  and  $\theta$  are shown in figure 6. Note that when  $\theta = \frac{3}{4}\pi$  there should be no coupling between  $A$  and  $B$ . Indeed  $B_0 / A_0$  approaches zero as

$$\frac{B_0}{A_0} \rightarrow \frac{\cos 2\theta}{2 \cos^2 \theta} \frac{\Omega_0}{\Omega}. \quad (4.10)$$

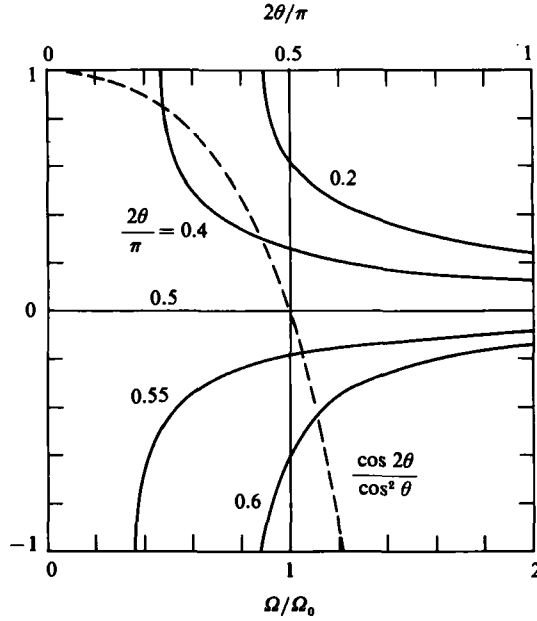


FIGURE 6. Reflection coefficient  $R(0)$  at  $x = 0$  and for  $x < 0$  are shown by —: numbers by the curves are the values of  $2\theta/\pi$  where  $\theta =$  angle of incidence; abscissa at top of figure.  $\cos 2\theta/\cos^2 \theta$  as a function of  $2\theta/\pi$  is shown by ----: abscissa at bottom of figure.

For  $\theta \approx \frac{1}{2}\pi$  (glancing incidence) the cutoff frequency is high and reflection is nearly complete.

As in the case of normal incidence, the effect of periodically modulated wave groups can be obtained by adding another train of detuned waves, and is not pursued here.

### 5. Sandbars on a sloping beach

We now examine the case where the mean depth  $h$  varies slowly with  $x$ . To enable analytical results, only normal incidence  $\theta = 0$  and perfectly tuned waves will be treated. Now the incident- and reflected-wave amplitudes  $A(x)$  and  $B(x)$  only vary slowly in  $x$ . We have from (2.36) and (2.37) that

$$A' + \frac{AC'_g}{2C_g} = \frac{-i\Omega_0 B}{C_g}, \quad (5.1a)$$

$$B' + \frac{BC'_g}{2C_g} = \frac{i\Omega_0 A}{C_g}, \quad (5.1b)$$

where  $\Omega_0$  and  $C_g$  are functions of  $x$ . Let

$$\bar{A} = AC_g^{\frac{1}{2}}, \quad \bar{B} = BC_g^{\frac{1}{2}}. \quad (5.2a, b)$$

Equations (5.1a, b) then become

$$\bar{A}' = \frac{-i\Omega_0 \bar{B}}{C_g}, \quad \bar{B}' = \frac{i\Omega_0 \bar{A}}{C_g}, \quad (5.3a, b)$$

which can be combined to give

$$\left(\frac{\bar{B}' C_g}{\Omega_0}\right)' = \frac{\Omega_0 \bar{B}}{C_g}. \quad (5.4)$$

Let the sandbars be confined to the region  $-L < x < 0$  and let the shoreline lie along  $x = L_0$  to the right of the bars. From the usual theory of refraction  $\bar{A}$  at  $x = -L$  is easily calculated from  $\bar{A}(-\infty)$ , and can be regarded as an input; this implies the boundary condition

$$\bar{B}' = i\Omega_0 \bar{A}/C_g \quad (x = -L). \quad (5.5)$$

Assume that all waves transmitted past the bars destroy themselves by breaking at the shoreline; we then have

$$\bar{B} = 0, \quad x = 0. \quad (5.6)$$

For any given  $h(x)$  and  $D(x)$  one can find  $k(x)$  for each  $\omega$  through the dispersion relation and then solve (5.3)–(5.5) numerically for any frequency. We shall however prescribe  $C_g/\Omega_0$  as a simple function of  $x$  to achieve analytical results. From (2.29) and (2.30) it can be shown that  $C_g/\Omega_0$  is monotonic in  $kh$  with the following limits:

$$\frac{C_g}{\Omega_0} \rightarrow \frac{4(gh)^{1/2}h}{\omega D} \rightarrow 0 \quad \text{as } kh \rightarrow 0, \quad (5.7)$$

$$\frac{C_g}{\Omega_0} \rightarrow \frac{g^2 e^{2kh}}{\omega^4 D} \rightarrow \infty \quad \text{as } kh \rightarrow \infty. \quad (5.8)$$

We assume a variation that is also monotonic:†

$$\frac{C_g}{\Omega_0} = \left(\frac{C_g}{\Omega_0}\right)_{-L} \frac{L_0 - x}{L_0 + L} \quad (-L < x < L_0). \quad (5.9)$$

In principle one can find the corresponding  $h(x)$  for a given  $\omega$  and  $D(x)$ . Note, however, that a different  $\omega$  gives rise to a different depth profile. Introducing the normalized quantities

$$X = \frac{x}{L}, \quad l = \frac{L_0}{L}, \quad (5.10)$$

we may rewrite (5.4) as

$$[(l-X)\bar{B}']' = \left(\frac{\Omega_0 L}{C_g}\right)_{-L}^2 \frac{(1+l)^2}{l-X} \bar{B} \quad (-1 < X < 0), \quad (5.11)$$

with the boundary conditions

$$\bar{B}' = i\bar{A} \left(\frac{\Omega_0 L}{C_g}\right)_{-L} \quad (X = -1), \quad (5.12)$$

$$\bar{B} = 0 \quad (X = 0), \quad (5.13)$$

where  $\bar{B}' \equiv d\bar{B}/dX$ . Equation (5.11) is equidimensional and can be easily solved:

$$\frac{\bar{B}(X)}{\bar{A}(-1)} = -i \frac{(l+1)^n (l-X)^{2n} - l^{2n}}{(l+1)^{2n} + l^{2n}}, \quad (5.14)$$

where

$$n = (1+l) \left(\frac{\Omega_0 L}{C_g}\right)_{-L}. \quad (5.15)$$

The reflection coefficient can be defined as

$$R = \left(\frac{\bar{B}}{\bar{A}}\right)_{-L} = \left(\frac{B}{A}\right)_{-L} = -i \frac{(l+1)^{2n} - l^{2n}}{(l+1)^{2n} + l^{2n}}. \quad (5.16)$$

†  $D(-L) \neq 0$  is assumed, otherwise a slight modification in the normalization is required.



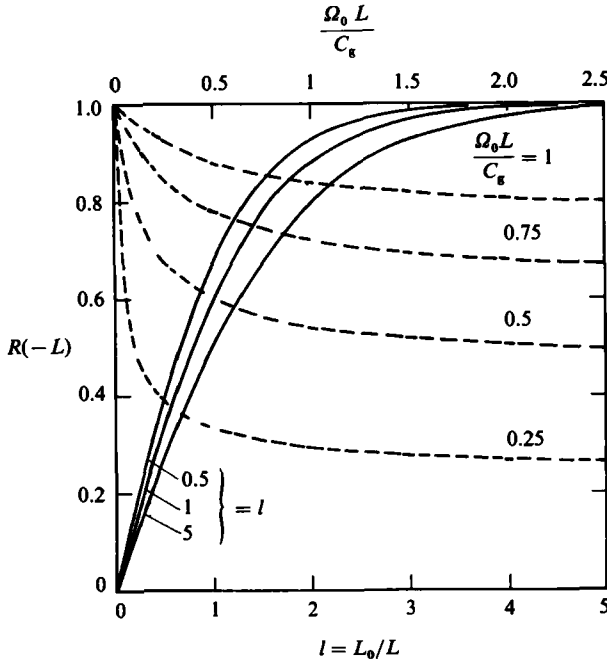


FIGURE 7. Reflection coefficient  $R(-L)$  of a sandbar patch on a sloping beach. For — (----) refer to top (bottom) of figure for abscissa.

For a fixed  $(\Omega_0 L/C_g)_{-L}$  the limit of  $l \gg 1$  corresponds to a horizontal bottom. Using the fact that

$$\lim_{l \rightarrow \infty} \left(1 + \frac{1}{l}\right)^l = e = 2.71828, \tag{5.17}$$

we get

$$\lim_{l \rightarrow \infty} R = -i \tanh \frac{\Omega_0 L}{C_g}, \tag{5.18}$$

which agrees with (3.21) at  $x = 0$ . When  $(\Omega_0 L/C_g)_{-L}$  is fixed but  $l \rightarrow 0$  (short beach),  $R$  approaches unity and the reflection is total. Figure 7 shows the dependence of  $R$  on  $(\Omega_0 L/C_g)_{-L}$  and  $l$ .

### 6. Mean sea level due to a detuned or a periodically modulated wavetrain

Through nonlinear convective inertia, surface waves give rise to radiation stresses in the mean, which in turn induce a mean sea level  $\zeta$  varying slowly in time and space. For infinitesimal waves  $\zeta$  is second order in wave slope. We limit our attention to normal incidence, constant mean depth, and long scales in both  $x$  and  $t$ . The equation governing  $\zeta$  is then

$$gh \frac{\partial^2 \zeta}{\partial x^2} - \frac{\partial^2 \zeta}{\partial t^2} = -\frac{1}{\rho} \frac{\partial^2 \mathcal{S}}{\partial x^2}, \tag{6.1}$$

after averages are taken with respect to depth and to  $x$  and  $t$  on the wave period of

the primary wave. When there are right- and left-going waves, it is easy to compute the pertinent radiation stress

$$\mathcal{S} = \frac{\rho g}{4} \frac{2C_g}{C} (|A|^2 + |B|^2), \tag{6.2}$$

where  $C = \omega/k$ .

We only consider a semi-infinite bar field,  $L \rightarrow \infty$ .

First let there be a train of slightly detuned incident waves. If  $\Omega/\Omega_0 > 1$  we get from (3.31)

$$|A|^2 + |B|^2 = |A_0|^2 + |B_0|^2 = |A_0|^2 \left\{ 1 + \left[ \frac{\Omega}{\Omega_0} + \left[ \left( \frac{\Omega}{\Omega_0} \right)^2 - 1 \right]^{\frac{1}{2}} \right]^{-2} \right\}, \tag{6.3}$$

which is constant in  $x$  and  $t$ . There the mean sea level is a constant setdown for both  $x \geq 0$ :

$$\bar{\zeta} = \frac{|A_0|^2}{2h} \frac{C_g}{C} \left\{ 1 + \left[ \frac{\Omega}{\Omega_0} + \left[ \left( \frac{\Omega}{\Omega_0} \right)^2 - 1 \right]^{\frac{1}{2}} \right]^{-2} \right\}. \tag{6.4}$$

The curly bracket above decreases from 2 to 1 as  $\Omega/\Omega_0$  increases from 1 to  $\lambda$ . If  $\Omega/\Omega_0 < 1$  we get similarly

$$\bar{\zeta} = -\frac{|A_0|^2}{h} \frac{C_g}{C} \begin{cases} 1 & (x < 0), \\ e^{-2Qx} & (x > 0), \end{cases} \tag{6.5a), (6.5b)}$$

where  $Q$  is given by (3.16). Use has been made of the fact that  $B_0/A_0 = R$  has unit magnitude (see (3.34)). Thus the mean sea level penetrates only half as far as the shorter waves.

Next let the incident-wave envelope be periodically modulated,

$$A = A_0 e^{iKx - i\Omega t} + * \quad (A_0 \text{ real}). \tag{6.6}$$

On the incidence side we have

$$|A|^2 + |B|^2 = 2(|A_0|^2 + |B_0|^2) + A_0^2 e^{2i(Kx - \Omega t)} + B_0^2 e^{-2i(Kx + \Omega t)} + *. \tag{6.7}$$

Consider first  $\Omega/\Omega_0 < 1$ . We have over the bars

$$|A|^2 + |B|^2 = 2(|A_0|^2 + |B_0|^2) + (A_0^2 + B_0^2) e^{-2Qx} e^{-i\Omega t} + *. \tag{6.8}$$

Clearly  $\bar{\zeta}$  consists of two parts:

$$\bar{\zeta} = \bar{\zeta}_0 + (\bar{\zeta}_2 e^{-2i\Omega t} + *). \tag{6.9}$$

The zeroth harmonic  $\bar{\zeta}_0$  is just twice the mean setdown given by (6.5a, b). The second harmonic  $\bar{\zeta}_2$  now represents long waves. Let us define

$$\bar{\zeta}_2 = \bar{\zeta}_P + \bar{\zeta}_H, \tag{6.10}$$

where  $\bar{\zeta}_P$  is the particular solution to (6.1) in response to the second-harmonic forcing in (6.7) and (6.8), while  $\bar{\zeta}_H$  is the homogeneous solution to (6.1). It is straightforward to show that

$$\bar{\zeta}_P = \frac{g}{C_g^2 - gh} \frac{C_g}{C} (A_0^2 e^{2iKx} + B_0^2 e^{-2iKx}) \quad (x < 0) \tag{6.11}$$

and 
$$\bar{\zeta}_P = -\frac{1}{h} \frac{C_g}{C} \frac{Q^2}{Q^2 + K^2} (A_0^2 + B_0^2) e^{-2Qx} \quad (x > 0). \tag{6.12}$$

The homogeneous solution owes its existence to the edge ( $x = 0$ ) of the bar field, as  $\bar{\zeta}_P$  alone cannot satisfy continuity requirements at  $x = 0$ . It may be written

$$\bar{\zeta}_H = N_{\pm} \exp\left(\pm 2i\Omega \frac{x}{(gh)^{\frac{1}{2}}}\right) \quad (x \geq 0), \quad (6.13)$$

which propagates at the long-wave velocity  $(gh)^{\frac{1}{2}}$  outwards to  $x \rightarrow \pm \infty$ . The constant amplitudes  $N_+$  and  $N_-$  can be determined by requiring the continuity of  $\bar{\zeta}_H + \bar{\zeta}_P$  and its  $x$ -derivative at  $x = 0$ . The result is

$$\frac{\pm N_{\pm}}{A_0^2/h} = \frac{C_g}{C} \left\{ \left(1 + \frac{B_0^2}{A_0^2}\right) \left[ \frac{Q^2}{Q^2 + K^2} \left(1 \pm i \frac{(gh)^{\frac{1}{2}}}{\Omega} Q\right) - \frac{1}{1 - C_g^2/gh} \right] \mp \left(1 - \frac{B_0^2}{A_0^2}\right) \frac{K(gh)^{\frac{1}{2}}}{\Omega(1 - C_g^2/gh)} \right\}. \quad (6.14)$$

Making use of (3.16) and (3.33), we find

$$\frac{\pm N_{\pm}}{A_0^2/h} = \frac{C_g}{C} e^{-i\psi} \left\{ \cos \psi \left[ \left(1 - \frac{\Omega^2}{\Omega_0^2}\right) \left[ 1 \pm i \frac{(gh)^{\frac{1}{2}}}{C_g} \frac{\Omega_0}{\Omega} \left[ 1 - \left(\frac{\Omega}{\Omega_0}\right)^2 \right]^{\frac{1}{2}} \right] - \frac{1}{1 - C_g^2/gh} \right] \mp i(\sin \nu) \frac{(gh)^{\frac{1}{2}}}{C_g(1 - C_g^2/gh)} \right\}, \quad (6.15)$$

where  $\nu$  is the phase of the complex reflection coefficient

$$\nu = \tan^{-1} \left\{ \left[ 1 - \left(\frac{\Omega}{\Omega_0}\right)^2 \right]^{\frac{1}{2}} / \frac{\Omega}{\Omega_0} \right\}. \quad (6.16)$$

In the limit  $kh \rightarrow 0$  we have

$$k|N_{\pm}| = \left(\frac{A_0}{kh^2}\right)^2. \quad (6.17)$$

In general the equal amplitude of  $N_+$  and  $N_-$  depends on  $kh$  and  $\Omega/\Omega_0$  and can be easily computed if desired. The important point here is that while the shorter surface waves are completely reflected to the left of the bars and only penetrate to a limited distance into the bar field, these long waves, which are distinct from the setup or setdown waves propagating at the group velocity of the short waves, are radiated and propagated at the fastest speed  $(gh)^{\frac{1}{2}}$  across the bar field without attenuation.† Thus along the shoreline protected by a large number of longshore bars, *infragravity* waves can be more dominant than the short waves. This dramatic filtering effect deserves experimental study.

Similar analysis can be carried out for the case  $\Omega/\Omega_0 > 1$ . Now there is only the particular solution

$$\bar{\zeta}_2 = \bar{\zeta}_P = -\frac{g}{gh - C_g^2} \frac{C_g}{C} \left\{ \begin{array}{l} (A_0^2 + B_0^2) e^{2iPx} \quad (x > 0), \\ A_0^2 e^{2iKx} + B_0 e^{-2iKx} \quad (x < 0), \end{array} \right\} \quad (6.18)$$

where  $P$  is defined by (4.7). On the left of the bar field, long waves are locked to the incident and reflected envelopes. Over the bars, long waves propagate at the speed which is always higher than  $C_g$ , as given by (3.32).

† Similar radiation of these long waves was also discussed for slowly varying sea depth by Mei & Benmoussa (1984).

## 7. Concluding remarks on sandbar initiation

The results in §§3 (case iii) and 5 now provide a theoretically consistent prediction of significant reflection which can initiate new offshore sandbars through mass transport, once there are already enough bars on the beach. We must now turn to the remaining question: what can be responsible for these old sandbars in the first place? One possibility is that the beach slope at the shoreline is much steeper than that offshore. A second possibility seems to lie with the breakpoint bar, which owes its existence to the plunging breakers. For a crude but quantitative estimate we apply the linearized shallow-water theory to a model bottom, which consists of a rectangular bar of depth  $h_1$ , followed immediately on its right by a rectangular trough of depth  $h_2$ . The depth elsewhere is  $h_0$  with  $h_1 < h_0 < h_2$ , while the widths of the bar and of the trough are both equal to  $a$ . For a normally incident wave from  $x \sim -\infty$  the reflection coefficient is found, after some algebra, to be

$$R = (1 - 4/\Delta)^{\frac{1}{2}}, \quad (7.1)$$

where

$$\begin{aligned} \Delta = & (2 \cos k_1 a \cos k_2 a)^2 + \left[ \left( \frac{h_2 + h_1}{h_1} \right) \sin k_1 a \sin k_1 a \right]^2 \\ & + \left[ \left( \frac{h_1 + h_0}{h_0} \right) \sin k_1 a \cos k_2 a + \left( \frac{h_2 + h_0}{h_0} \right) \sin k_2 a \cos k_1 a \right]^2 \\ & - \left( \frac{h_2 + h_1}{h_1} \right) \sin 2k_1 a \sin 2k_2 a, \end{aligned} \quad (7.2)$$

with

$$k_1 = \frac{\omega}{(gh_1)^{\frac{1}{2}}}, \quad k_2 = \frac{\omega}{(gh_2)^{\frac{1}{2}}}. \quad (7.3)$$

Note that on the side  $x > 0$  no left-going waves (reflection from the beach) are allowed.

Take for example  $\omega = 2\pi/T = 1 \text{ s}^{-1}$ ,  $h_0 = 1 \text{ m}$ ,  $h_1 = 0.5 \text{ m}$ ,  $h_2 = 1.5 \text{ m}$  and  $a = 1 \text{ m}$ ; we find  $R = 0.43$ , which is sufficiently great for the convergence of mass transport, as mentioned in §1. Needless to say this estimate suffers from the shortcomings of both linearization and idealized topography. Its order of magnitude, however, is probably correct. Thus a breakpoint bar can provide sufficient reflection to start the first few bars; the mechanism of resonant reflection described in this paper then reinforces the tendency and induces still more bars offshore.

On a natural beach, the mechanism proposed here may only be one phase of an evolving process. Seasonal variation of the wave climate or the arrival of a storm can heighten the importance of nonlinearity; the simple linearized description may no longer suffice. If waves break over the bars, the bar crests can be eroded, and the tendency of bar formation can be altered. These features deserve further studies.

The present research is supported by the Office of Naval Research (contract N00014-83K-0550) and the National Science Foundation (grant MEE 821-0649).

## REFERENCES

- CARTER, T. G., LIU, P. L-F. & MEI, C. C. 1973 Mass transport by waves and offshore sand bedforms. *J. Waterways, Harbours, Coastal Engng Div. ASCE* **99**, 165-184.
- CRAIK, A. D. D. & ADAM, J. A. 1978 Evolution in space and time of resonant wave triads. *Proc. R. Soc. Lond. A* **363**, 243-255.
- DAVIES, A. G. 1982 The reflection of wave energy by undulations on the seabed. *Dyn. Atmos. Oceans* **6**, 207-232.
- DOLAN, T. J. 1983 Wave mechanics for the formation of multiple longshore bars with emphasis on the Chesapeake Bay. M.S. thesis, Civil Engineering, University of Delaware.
- EVANS, O. F. 1940 The low and ball of the eastern shore of Lake Michigan. *J. Geol.* **48**, 476-511.
- HEATHERSHAW, A. D. 1982 Seabed-wave resonance and sandbar growth. *Nature* **296**, 343-345.
- HERBICH, J. B., MURPHY, H. D. & VAN WEELE, B. 1965 Scour of flat sand beaches due to wave action in front of sea walls. *Coastal Engineering: Santa Barbara Specialty Conf., ASCE*, pp. 705-726.
- JOHNS, B. 1970 On the mass transport induced by oscillatory flow in a turbulent boundary layer. *J. Fluid Mech.* **43**, 177-185.
- KEULEGAN, G. H. 1948 An experimental study of submarine sandbars. *Beach Erosion Board Tech. Rep. 3, U.S. Army Corps Engrs.* Reprinted in SCHWARZ, M. L. (ed.) 1972 *Spits and Bars*. Dowden, Hutchinson & Ross.
- KINDLE, E. M. 1936 Notes on shallow water sand structures. *J. Geol.* **44**, 861-869.
- LAU, J. & TRAVIS, B. 1973 Slowly varying Stokes waves and submarine longshore bars. *J. Geophys. Res.* **78**, 4489-4498.
- LONGUET-HIGGINS, M. S. 1953 Mass transport in water waves. *Phil. Trans. R. Soc. Lond. A* **345**, 535-581.
- LONGUET-HIGGINS, M. S. 1958 The mechanics of the boundary layer near the bottom in a progressive wave. In *Proc. 6th Conf. Coastal Engineering*, pp. 184-193.
- MCGOLDRICK, L. F. 1968 Long waves over wavy bottoms. *Office Nav. Res. Ocean Sci. Tech. Group Tech. Rep. 1*.
- MEI, C. C. 1983 *Applied Dynamics of Ocean Surface Waves*. Wiley-Interscience.
- MEI, C. C. & BENMOUSSA, C. 1984 Long waves induced by short-wave groups over an uneven bottom. *J. Fluid Mech.* **139**, 219-235.
- MITRA, A. & GREENBERG, M. D. 1984 Slow interaction of gravity waves and a corrugated seabed. *Trans. ASME E: J. Appl. Mech.* **51**, 251-255.
- NIELSEN, P. 1979 Some basic concepts of wave sediment transport. *Tech. Univ. Denmark, Inst. Hydrodyn. Hydraul. Engng Ser. Paper 20*.
- PINSKER, Z. G. 1978 *Dynamical Scattering of X-rays in Crystals*. Springer.
- RHINES, P. B. & BRETHERTON, F. P. 1973 Topographic Rossby waves in a rough-bottomed ocean. *J. Fluid Mech.* **61**, 583-607.
- SAYLOR, J. H. & HANDS, E. B. 1970 Properties of longshore bars in the Great Lakes. In *Proc. 12th Conf. Coastal Engineering*, vol. 2, pp. 839-853.
- SHEPPARD, F. P. 1950 Longshore bars and longshore troughs. *Beach Erosion Board Tech. Memo. 15, US Army Corps Engrs.* Reprinted in SCHWARZ, M. L. (ed.) 1972 *Spits and Bars*. Dowden, Hutchinson & Ross.
- SHORT, A. D. 1975 Multiple offshore bars along the Alaskan Arctic Coast. *J. Geol.* **83**, 209-211.
- TAGAKI, S. 1969 A dynamic theory of diffraction for a deformed crystal. *J. Phys. Soc. Japan* **27**, 1239-1253.
- ZENKOVICH, V. P. 1967 *Processes of Coastal Development*, pp. 219-236. Interscience.